TOXICOLOGICAL SCIENCES **109(2)**, 336–349 (2009)
doi:10.1093/toxsci/kfp070
Advance Access publication April 6, 2009

Comparative Analysis of Novel Noninvasive Renal Biomarkers and Metabonomic Changes in a Rat Model of Gentamicin Nephrotoxicity

Max Sieber,*,[1] Dana Hoffmann,*,[1] Melanie Adler,* Vishal S. Vaidya,† Matthew Clement,† Joseph V. Bonventre,† Nadine Zidek,* Eva Rached,* Alexander Amberg,‡ John J. Callanan,§ Wolfgang Dekant,* and Angela Mally*,[2]

*Department of Toxicology, University of Würzburg, 97078 Würzburg, Germany; †Renal Division, Department of Medicine, Brigham and Women's Hospital, Harvard Medical School, Boston, Massachusetts 02115; ‡Sanofi-Aventis, Drug Safety Evaluation, Hattersheim 65795, Germany; and §School of Agriculture, Food Science & Veterinary Medicine and Conway Institute of Molecular & Biomedical Research, University College Dublin, Dublin 4, Ireland

Received January 22, 2009; accepted March 27, 2009

Although early detection of toxicant induced kidney injury during drug development and chemical safety testing is still limited by the lack of sensitive and reliable biomarkers of nephrotoxicity, omics technologies have brought enormous opportunities for improved detection of toxicity and biomarker discovery. Thus, transcription profiling has led to the identification of several candidate kidney biomarkers such as kidney injury molecule (Kim-1), clusterin, lipocalin-2, and tissue inhibitor of metalloproteinase 1 (Timp-1), and metabonomic analysis of urine is increasingly used to indicate biochemical perturbations due to renal toxicity. This study was designed to assess the value of a combined ^{1}H-NMR and gas chromatography–mass spectrometry (GC-MS) metabonomics approach and a set of novel urinary protein markers for early detection of nephrotoxicity following treatment of male Wistar rats with gentamicin (60 and 120 mg/kg bw, sc) for 7 days. Time- and dose-dependent separation of gentamicin-treated animals from controls was observed by principal component analysis of ^{1}H-NMR and GC-MS data. The major metabolic alterations responsible for group separation were linked to the gut microflora, thus related to the pharmacology of the drug, and increased glucose in urine of gentamicin-treated animals, consistent with damage to the S_1 and S_2 proximal tubules, the primary sites for glucose reabsorption. Altered excretion of urinary protein biomarkers Kim-1 and lipocalin-2, but not Timp-1 and clusterin, was detected before marked changes in clinical chemistry parameters were evident. The early increase in urine, which correlated with enhanced gene and protein expression at the site of injury, provides further support for lipocalin-2 and Kim-1 as sensitive, noninvasive biomarkers of nephrotoxicity.

Key Words: **kidney; nephrotoxicity; biomarker; metabonomics; Kim-1; lipocalin-2.**

The kidney is one of the main target organs of xenobiotic induced toxicity. However, minor effects on renal function are difficult to detect due to the functional reserve of the kidney. So far, the most commonly used clinical markers of renal injury in routine toxicity studies remain blood urea nitrogen (BUN) and serum creatinine, but they suffer from lack of sensitivity, revealing kidney damage not until 70–80% of the renal epithelial mass has been lost. Because of these limitations, there is a need to establish more sensitive and reliable, preferably noninvasive markers, which may be used to detect toxicant induced kidney injury and monitor renal function during drug development and chemical safety testing.

Over the last years, a range of candidate biomarkers for kidney injury have emerged primarily from toxicogenomic studies, and several of these markers have also been shown to be released into urine in response to kidney damage, highlighting their potential to serve as noninvasive markers for nephrotoxicity detection. These include neutrophil gelatinase–associated lipocalin (NGAL, lipocalin-2), which has been shown to be rapidly induced and secreted into urine in a range of preclinical and clinical studies on acute kidney injury (Bennett *et al*., 2008; Mishra *et al*., 2004, 2006; Nickolas *et al*., 2008; Wheeler *et al*., 2008), clusterin, a secreted glycoprotein synthesized in response to tubular injury (Hidaka *et al*., 2002; Ishii *et al*., 2007; Kharasch *et al*., 2006; Yang *et al*., 2007), and kidney injury molecule (Kim-1), which has been demonstrated to be suitable for early prediction of graft loss in renal transplant recipients, adverse clinical outcome in patients with acute renal failure, and drug/chemical induced proximal tubule damage (Liangos *et al*., 2007; Prozialeck *et al*., 2007; van Timmeren *et al*., 2007; Zhou *et al*., 2008). Similarly, elevated levels of tissue inhibitor of metalloproteinases 1 (Timp-1) have been observed in models of kidney injury and in urine of patients with renal disease as compared to healthy controls (Chromek *et al*., 2003; Horstrup *et al*., 2002; Wasilewska and Zoch-Zwierz, 2008).

In addition to these protein markers, metabonomic approaches, that is, the multicomponent analysis of the biochemical composition of body fluids combined with statistical models, are

[1] These authors contributed equally to this study.

[2] To whom correspondence should be addressed at Department of Toxicology, University of Würzburg, Versbacher Strasse 9, 97078 Würzburg, Germany. Fax: +49-931-20148865. E-mail: mally@toxi.uni-wuerzburg.de.

increasingly being used in drug and chemical safety assessment to diagnose or predict toxicity (Lindon *et al.*, 2007). The principal analytical technique for global metabolic profiling has long been high field proton nuclear magnetic resonance (^{1}H-NMR) spectroscopy, and numerous studies indicate that ^{1}H-NMR based metabonomics can discriminate healthy and diseased, control and treated animals/individuals (Lienemann *et al.*, 2008; Odunsi *et al.*, 2005; Wei *et al.*, 2008). However, ^{1}H-NMR analysis is restricted to a limited number of high-concentration metabolites. An alternative approach is to use mass spectrometry (MS) based metabonomic techniques, which require separation of individual metabolites by either liquid chromatography (LC) or gas chromatography (GC), but offer greater sensitivity as compared to ^{1}H-NMR. Thus, GC-MS or LC-MS not only enable detection of low-concentration metabolites, but also hold promise for biomarker identification. However, it is important to recognize that ^{1}H-NMR spectroscopy and mass spectrometry are complementary tools and that a combination of methods provides wider coverage of metabolites and thus a much more comprehensive picture of the metabolome than any single technique by itself. Utilizing a combination of ^{1}H-NMR, GC-MS, and LC-MS techniques, Atherton *et al.* (2006) were able to identify metabolic perturbations in the PPAR-α null mutant mouse liver as compared with wild-type mice, ranging from decreased glucose and choline (^{1}H-NMR) to increased steric acid, cholesterol and pentadecanoic acid (GC-MS). Similarly, plasma analysis using all three analytical platforms provided a more comprehensive metabolite profile of normal and Zucker (fa/fa) obese rats than any methodology would have on its own. For instance, GC-MS revealed an increase in arachidonic acid and tocopherol, whereas a rise in taurocholate in Zucker rats was detected using ultra performance LC-MS (Williams *et al.*, 2006).

The aim of this study was to compare the sensitivity of a combined ^{1}H-NMR and GC-MS metabonomics approach and a set of novel urinary protein markers for early detection of chemically induced nephrotoxicity. The overall study design and choice of model compound, that is, the aminoglycoside antibiotic gentamicin, was based on a study by Lenz *et al.* (2005) in which LC-MS analysis of metabolic changes in rat urine revealed altered excretion of xanthurenic acid, kynurenic acid and various sulfate conjugates in addition to increased glucose, lactate and decreased betaine zand trimethylamine-*N*-oxide detected by ^{1}H-NMR, but an additional low dose and quantitative assessment of the major urinary metabolites detected by ^{1}H-NMR were included in our study to allow a comprehensive assessment of the sensitivity/specificity of metabolic changes and candidate urinary protein markers along with traditional markers of nephrotoxicity.

MATERIALS AND METHODS

Chemicals and solvents. All chemicals and reagents were purchased from commercial suppliers. Methoxyamine hydrochloride, dried pyridine, acetone, and chloroform were obtained from Sigma-Aldrich (Taufkirchen, Germany). Methanol was purchased from Carl Roth GmbH (Karlsruhe, Germany). N-methyl-N-(trimethylsilyl)-trifluoracetamide (MSTFA) was purchased from AppliChem (Darmstadt, Germany). Gentamicin was purchased as solution (5 × 50 mg/ml in deionized water, liquid, sterile-filtered, cell culture tested, Sigma-Aldrich (Lot no. 057K2371).

Animals and treatment. Male Wistar rats, 6–8 weeks old, weighing 200 g were purchased from Harlan-Winkelmann (Borchen, Germany) and were randomly divided into three groups of five animals. Animals were kept in Macrolon cages (five animals per cage) on a 12-h light/dark cycle and allowed free access to standard laboratory chow (SSniff, Soest, Germany) and tap water. Rooms were maintained at a temperature of 21 ± 2°C and humidity of 55 ± 10%. Following a week of acclimatization, animals were adjusted to metabolic cages 3 days prior to treatment.

Gentamicin dosing solutions of 10 mg/ml (low-dose group) and 20 mg/ml (high-dose group) were prepared daily by diluting the stock solution 1:5 or 1:2.5 with sterile water. Gentamicin at dose levels of 60 and 120 mg/kg bw per day was administered subcutaneously as two separate doses of 30 and 60 mg/kg bw, respectively, twice daily at an eight hour interval, for 7 consecutive days. Control groups received an equal volume of 0.9% physiological saline. The animals were housed in individual metabolic cages during the study. Body weight as well as food and water consumption were recorded daily. Urine was collected at 24-h intervals. A 250-µl aliquot of urine was used directly for clinical chemistry urine analyses. The remaining urine was aliquoted and stored at −20°C until further analysis. Blood samples were drawn from the retro-orbital plexus under light isoflourane anaesthesia 24 and 72 h after the first dosing and used for clinical biochemistry. At the end of the study, animals were sacrificed by CO_2 asphyxiation and blood was collected by cardiac puncture. Blood samples were collected into heparinized tubes and centrifuged. A 250-µl aliquot of plasma was used for clinical biochemistry analyses. The remaining plasma was stored at −20°C until further analysis. Organs (liver and kidney) were removed and weighed. Half of the left kidney and part of the left liver lobe were fixed in neutral buffered formalin and embedded into paraffin. The remaining kidney and liver tissue was aliquoted and snap-frozen in liquid nitrogen and stored at −80°C.

Clinical chemistry. Urine and plasma analyses were carried out at the Laboratory for Clinical Chemistry, University of Würzburg, on a Vitros 700XR (Ortho-Clinical Diagnostics, Neckarsgemuend, Germany) using standard protocols for the determination of these parameters according to manufacturer's instructions. The following parameters were determined in urine: glucose, GGT (γ-glutamyl transferase), total protein, creatinine, and osmolality. Blood samples were collected on days 1, 3, and 7 and the following parameters were determined in plasma: creatinine, urea, total bilirubin, aspartate aminotransferase, alanine amino transferase, GGT, alkaline phosphatase, and total protein.

Enzyme-linked immunosorbent assay. Urinary clusterin was determined using a commercially available Rat ELISA (enzyme-linked immunosorbent assay) Kit according to the manufacturer's instructions (Biovendor, Heidelberg, Germany). Urinary Kim-1 protein was measured in the Vaidya/Bonventre laboratories using Microsphere-based Luminex xMAP technology as described previously (Vaidya *et al.*, 2005, 2008). Timp-1 was determined using the rat TIMP-1 DuoSet ELISA Development System (R&D, Wiesbaden, Germany) according to the manufacturer's instructions. For quantification of urinary lipocalin-2, a sandwich ELISA was developed using two monoclonal antibodies (BioPorto Diagnostics, Gentofte, Denmark). Microtiter plates (Nunc-Immuno Maxisorp, Denmark) were coated overnight at 4°C with purified mouse anti-rNGAL (125 ng per well) in carbonate buffer (0.1 M Na_2CO_3/$NaHCO_3$, pH 9.6). After repeated washing with PBST (phosphate-buffered saline supplemented with 0.05% Tween-20, pH 7.4), nonspecific protein binding sites were blocked by incubating with 1% bovine serum albumin in PBS (200 µl per well) for 2 h at room temperature. After washing, 100 µl of urine (diluted 1:1600 or 1:6400) or standards (recombinant rNGAL in a concentration range 156.3–5000 pg/ml) were added to the wells and incubated for 2 h at room temperature. Following several washing steps, bound antigens were detected by addition of biotinylated anti-rNGAL antibody diluted 1:4000 for 90 min and streptavidin-horseradish peroxidase (Vector Laboratories, Burlingame, CA) for 30 min at room

temperature. Finally, peroxidase activity was determined using the chromogenic substrate TMB (3,3′,5,5′-tetramethylbenzidine, 30 min). The reaction was stopped by the addition of 100 µl of 1M sulfuric acid (Sigma-Aldrich) and absorbance was measured using SpectraMax 190 microplate reader (Molecular Devices, Sunnyvale, CA) at 450 nm. Intra- and interassay variation coefficients were < 6.19 ($n = 8$) and < 9.38 ($n = 4$), respectively.

Immunohistochemistry. Kidney sections (5 µm) were prepared from formalin fixed, paraffin embedded tissue blocks and mounted onto glass slides. Sections were deparaffinized, rehydrated, and washed in PBS. Heat-induced antigen retrieval was achieved by 4-min autoclaving in 10mM citrate buffer, pH 6.0. For detection of Timp-1 and lipocalin-2/NGAL, tissues were then treated with 0.1% trypsin for 2 min at 37°C. After washing in PBS, sections were blocked with 5% donkey serum in PBS for 1 h. Endogenous peroxidase was subsequently blocked by incubation with 3% H_2O_2 in PBS for 10–15 min, followed by two additional blocking steps with 0.001% avidin in PBS for 15 min and 0.001% biotin in PBS for 15 min, with several wash steps in between. Sections were incubated with primary antibodies diluted in 5% donkey serum in PBS overnight at 4°C. Antibodies were applied in the following concentrations: anti-clusterin (goat polyclonal, Santa Cruz, Heidelberg, Germany) 1 µg/ml; anti-lipocalin-2 (goat polyclonal, R&D Systems, Wiesbaden, Germany) 1.3 µg/ml; anti-Kim-1 (goat polyclonal, R&D Systems) 0.5–1 µg/ml; anti-Timp-1 (rabbit polyclonal, Acris Antibodies, Hiddenhausen, Germany) 2.5 µg/ml. After three wash steps, tissues were incubated with the biotinylated secondary antibody (donkey anti-goat IgG or goat anti-rabbit IgG, Santa Cruz, Heidelberg, Germany), diluted 1:200 in PBS for 45 min at room temperature and subsequently washed with PBS. Following 30-min incubation with the complex of avidin and biotinylated horseradish peroxidase, enzyme activity was visualized using 3,3′-diaminobenzidine. Tissues were counterstained with hematoxylin, dehydrated, and mounted in Eukitt mounting medium (Sigma-Aldrich).

Quantitative RT-PCR. RNA was isolated from aliquots of frozen kidney using the TRIR total RNA isolation reagent (ABgene, Hamburg, Germany) and further purified using the RNeasy Mini Kit (Qiagen GmbH, Hilden, Germany) according to manufacturer's instructions, including DNase treatment. Purified RNA was quantified by measuring the absorbance at 260 nm. RNA integrity was quality controlled by electrophoresis on a 1.2% formaldehyde agarose gel. Purified RNA samples were stored at −80°C until use. cDNA was synthesized from 1 µg RNA using the first Strand Synthesis Kit (ABgene), diluted 1:5 with H_2O and stored at −20°C. Quantitative real-time PCR was performed using the Roche Lightcycler 480 (Roche, Mannheim, Germany) in 25-µl reactions containing 2× mastermix with SYBR Green I (ABgene), 2.5 µl of cDNA and 70nM of each primer. Amplification was carried out using the following temperature profile: 15-min enzyme activation at 95°C, followed by 40 cycles of 95°C for 15 s, 60°C for 30 s, and 72°C for 30 s. Primer sequences for target and reference genes were as previously described (Rached *et al*., 2008). PCR product formation was determined by measuring the fluorescence signal emitted by the incorporation of SYBR Green I into double stranded DNA. Using standard curves, amplification efficiencies of both endogenous reference gene (β-actin) and target genes were assessed. Product specificity was examined by melting curve analysis and electrophoresis on a 5% polyacrylamide gel.

Gene expression changes relative to untreated controls were determined by the $2^{-\Delta\Delta Ct}$ method (see "Critical factors for Successful Real-time PCR," Qiagen). Samples were amplified in duplicate and normalized against β-actin. Results are presented as mean fold change in mRNA expression of five animals per dose group compared with control animals.

GC-MS analysis. Urine samples were thawed overnight at 4°C. After thawing, samples were briefly vortexed, and proteins were precipitated by addition of 100 µl of ice-cold methanol to 50 µl of urine. After centrifugation (10,000 × g, 10 min), 50 µl of the supernatant were transferred to a GC autosampler vial with a micro insert. Repeated analysis of a pooled sample for quality control was proposed by Sangster *et al*. (2006) to overcome the problem of monitoring sample preparation and analytical performance in untargeted analyses, where internal standards cannot be implemented easily. Thus, aliquots of 50 µl from each sample were pooled and vortexed. Aliquots (50 µl) of this pooled urine were transferred into GC autosampler vials with micro inserts to serve as quality control. The number of quality controls was chosen to account for ~20% of all samples analyzed. Quality control samples were subsequently treated in the same manner as the samples. The samples were evaporated to dryness at 30°C in a Centrivac vacuum centrifuge (Heraeus Instruments, Osterode, Germany). After 2 h, 50 µl of acetone were added to each sample to ensure complete drying of the sample. Acetone addition was repeated once. After drying, the samples were derivatized with 50 µl of methoxyamine hydrochloride in pyridine (20 mg/ml) at 40°C for 90 min. Then, samples were silylated at 40°C for 1 h with 100 µl of MSTFA. All samples and quality controls were randomized for each treatment step.

Samples were analyzed on a HP6980 gas chromatograph with split inlet (split ratio 20:1) equipped with a J&W Scientific DB5-MS column (dimensions: 30 m × 0.25 mm × 0.1 µm film) coupled to a HP5973 mass selective detector. Data recording and instrument control was performed by HP ChemStation version D.02.00 (all from Agilent GmbH, Waldbronn, Germany). Samples were introduced by a CombiPal autosampler (CTC Analytics GmbH, Zwingen, Switzerland). Inlet temperature and transfer line temperature were set to 280°C. The oven temperature increased from 60°C to 85°C at a rate of 2.5°C/min and from 85 to 280°C at a rate of 9.0°C/min and was then held at 280°C for 4 min. Total run time was 35.6 min. Helium carrier gas flow was kept constant at 0.8 ml/min. The MS detector was switched off during the elution of the urea signal from 11.50 min to 16.00 min. The detector operated in the scan mode from 60 *m/z* to 650 *m/z* with a sampling rate of 1 leading to 8.69 scans/s and a threshold of 50 counts. Source temperature and quadrupole temperature was kept at 230 and 150°C, respectively.

Chromatograms were inspected visually and those that deviated strongly from the pooled quality controls due to chromatographic problems such as poor resolution, no peaks present etc. were excluded. Such samples carry no information for the following statistical analysis and interfere with the automated peak picking and alignment process. The remaining samples were exported in the platform-independent netCDF (*.cdf) format with the HP ChemStation export function for further analysis. Automated peak detection and peak alignment was performed by the XCMS software. R-program version 2.4.0 (R-Foundation for statistical computing, www.R-project.org) and XCMS version 1.6.1 (Want *et al*., 2006) were used. Default parameters of XCMS were used except for the following: full width at half-maximum = 4.0 s, profmethod = "binlinbase." The results table containing mass spectral features as mass/retention time pairs in a tab-separated text file (*.txt) was imported into Excel work sheets (Microsoft, Unterschleißheim, Germany). Normalization to total ion current and further data handling steps such as sorting the data according to retention time was carried out in Excel prior to statistical analysis with SIMCA-P+ version 11.5 (Umetrics, Umeå, Sweden). Variables were mean-centered and pareto-scaled for PCA and orthogonal projection to latent structures discriminant analysis (OPLS-DA). The significance of the components was determined by leave-one-out cross validation, the default validation tool in SIMCA. Only significant components were used for the analysis. If a separation between control and dose groups was observed in the PCA scores plot, OPLS-DA was performed to highlight the differences between the groups. Potential markers for group separation were identified by analyzing the S-plot (Wiklund *et al*., 2007) which plots the covariance (p) of the discriminating component $t[1]P$ against its correlation (p(corr)), using a cut-off value of $p \geq |0.05|$ and $p(\text{corr}) \geq |0.5|$. The potential markers were located on the outer ends of the S-shaped point swarm. Markers were selected in a conservative manner so that only those markers showing a significant jack-knifed confidence interval of less than half of the variable's covariance p were further investigated. With the mass/retention time pairs, the corresponding peak was identified in the original GC chromatograms. Then, AMDIS deconvolution was run and the peak was compared with the NIST mass spectral database for identification (National Institute of Standards and Technology, Gathersburg, MD). Confirmation of peak identity was carried out by coeluting authentic reference compounds, if available.

^{1}H-NMR analysis. Urine samples were thawed overnight at 4°C and precipitated solids were removed by centrifugation (10,000 × g, 10 min). Urine (630 µl) was buffered with 70 µl of a 1M phosphate buffer in D_2O containing 10mM d_4-trimethylsilylpropionic acid sodium salt (TSP) as shift lock reagent

TABLE 1
Body Weight and Clinical Chemistry Parameters in Response to Gentamicin Treatment

		Urine						Plasma	
Dose (mg/kg bw)	Body weight (g)	Volume (ml/24 h)	Osmolarity (mosmol/kg)	Creatinine (mg/24 h)	Glucose (mg/24 h)	GGT (U/24 h)	Total protein (mg/24 h)	Creatinine (mg/dl)	Urea (mg/dl)
Day 1									
0	234 ± 3	11.4 ± 2.4	1457 ± 385	5.6 ± 0.7	28.6 ± 3.6	936 ± 238	11.3 ± 4.9	0.2 ± 0.0	37.5 ± 3.8
60	230 ± 12	8.2 ± 2.2*	1477 ± 147	5.6 ± 0.7	28.2 ± 3.4	1513 ± 276*	12.0 ± 3.8	0.2 ± 0.0	43.7 ± 1.5
120	226 ± 3	8.0 ± 1.2*	1728 ± 370	5.9 ± 0.5	62.1 ± 23.7**	1534 ± 527**	14.4 ± 3.1	0.2 ± 0.0	46.0 ± 9.3
Day 2									
0	236 ± 3	10.0 ± 1.6	1568 ± 411	5.4 ± 0.5	25.4 ± 2.6	1273 ± 185	10.7 ± 4.1	n.d.	n.d.
60	232 ± 12	6.6 ± 1.1	1615 ± 327	4.9 ± 0.9	35.1 ± 5.9	1939 ± 385	9.9 ± 4.2	n.d.	n.d.
120	224 ± 6	7.5 ± 3.8	1563 ± 717	5.2 ± 0.3	51.1 ± 9.9***	2442 ± 585	12.6 ± 3.2	n.d.	n.d.
Day 3									
0	239 ± 4	10.6 ± 2.9	1551 ± 347	5.7 ± 0.8	24.3 ± 3.2	1451 ± 343	10.4 ± 3.4	0.2 ± 0.0	38.1 ± 6.8
60	237 ± 16	8.8 ± 1.7	1472 ± 165	5.0 ± 0.7	30.7 ± 5.2	1633 ± 432	9.5 ± 0.7	0.2 ± 0.0	42.4 ± 4.9
120	224 ± 7	10.4 ± 3.4	1216 ± 500	5.5 ± 0.8	40.0 ± 10.5*	1757 ± 522	13.6 ± 4.7	0.3 ± 0.1*	50.2 ± 5.5*
Day 6									
0	247 ± 6	9.6 ± 3.3	1959 ± 614	6.1 ± 1.0	30.7 ± 9.7	1535 ± 368	12.7 ± 5.3	0.2 ± 0.0	39.2 ± 4.1
60	239 ± 21	14.4 ± 4.2	1171 ± 434*	6.2 ± 0.5	194.8 ± 308.3	2015 ± 475	24.6 ± 7.5	0.6 ± 0.6	89.6 ± 54.6
120	206 ± 12**	12.0 ± 6.2	377 ± 61***	2.7 ± 1.1***	262.8 ± 245.2	622 ± 528	28.2 ± 16.2	5.0 ± 1.6***	496.3 ± 145.5***

Note. Data are presented as mean ± SD ($n = 5$). Statistical analysis was performed by ANOVA and Dunnett's *post hoc* test. Statistically significant changes compared with controls are indicated as *$p < 0.05$, **$p < 0.01$, and ***$p < 0.001$. n.d., not determined.

prior to transfer into a 5-mm NMR tube (Aldrich Series 30). Samples were randomized for each treatment step. Spectra were recorded on a Bruker DMX 600 spectrometer equipped with a 5-mm dual carbon-proton cryoprobe using pulsed magnetic field gradients (both by Bruker Biospin GmbH, Rheinstetten, Germany). Water suppression was achieved with the noesygppr1d pulse sequence from the Bruker library. For Fourier transformation, 32 scans were recorded. Each spectrum was manually baseline-corrected and referenced to TSP ($\delta = 0.00$ ppm). Instrument control, data recording, and baseline correction was carried out with the Bruker WIN-NMR Suite. Spectra were inspected visually to exclude any outliers due to dilute samples or inadequate water suppression. The spectra were then imported into the Chenomx NMR Suite 5.1 (Chenomx, Edmonton, Canada) and binned into 0.04 ppm wide bins. The bins around the water resonance from 4.40 to 6.20 ppm were excluded from the analysis. Binned ^{1}H-NMR data were normalized to total integral and imported into SIMCA-P+ version 11.5. Multivariate data analysis was carried out in the same manner as described for the GC-MS data. The compounds contained in the bins which were found to be altered due to gentamicin treatment were identified and quantified using the spectral library of the Chenomx NMR Suite. Quantification was carried out by overlaying the sample signals with the reference signals contained in the spectral library and comparing spectral peak areas to the TSP reference signal.

Statistical analyses. Unless otherwise indicated, data are presented as mean ± SD. Statistical analyses were conducted by ANOVA followed by Dunnett's *post hoc* test. Receiver operator characteristics (ROC) curves were plotted by entering data obtained from control versus treated animals on days 1, 3, and 6, respectively days 1, 3, and 7 for parameters measured in serum, using the Graph Pad Prism 5 software package (GraphPad Software, Inc., La Jolla, CA).

RESULTS

General Toxicity, Histopathology, and Clinical Chemistry

Treatment with gentamicin at a daily dose of 120 mg/kg bw resulted in a significant decrease in body weight by day 6 (Table 1) and concomitant increase in relative kidney weight as compared to control animals (0.81 ± 0.07 g/kg bw in controls vs. 0.93 ± 0.06 and 0.97 ± 0.11 g/kg bw in low and high-dose animals, respectively). Two high-dose animals were removed from the study on day 6 due to overt signs of toxicity. Kidneys of both low (60 mg/kg bw) and high-dose group animals (120 mg/kg bw) appeared pale and microscopic evaluations of renal tissue confirmed the presence of epithelial necrosis, predominantly involving proximal convoluted tubules of the cortex, with increasing severity related to dose (Fig. 1). In animals treated with gentamicin at 60 mg/kg bw, histopathological changes varied from complete loss of tubular cells to tubules containing cells with pyknotic, karyorrhectic, and karyolitic nuclei. Necrosis and loss of proximal tubule lining cells was graded primarily as mild (2/5) to moderate (2/5), although one low-dose animal (1/5) also showed a more extensive proximal tubule necrosis. Multifocal interstitial mononuclear cell infiltrations were observed in 2/5 low-dose animals. Extensive necrosis and loss of proximal tubule lining cells was evident in 5/5 animals treated with gentamicin at 120 mg/kg bw. These changes were accompanied by proteinaceous casts in some tubules, but no significant inflammation associated with regions of necrosis was noted.

In high-dose animals, a small but statistically significant increase in serum creatinine and blood urea nitrogen was evident from day 3 on, consistent with a decrease in urinary creatinine excretion at later time points (Table 1), whereas no changes were observed in rats treated with the low dose of 60 mg/kg bw. Significant changes in urinary glucose indicative of

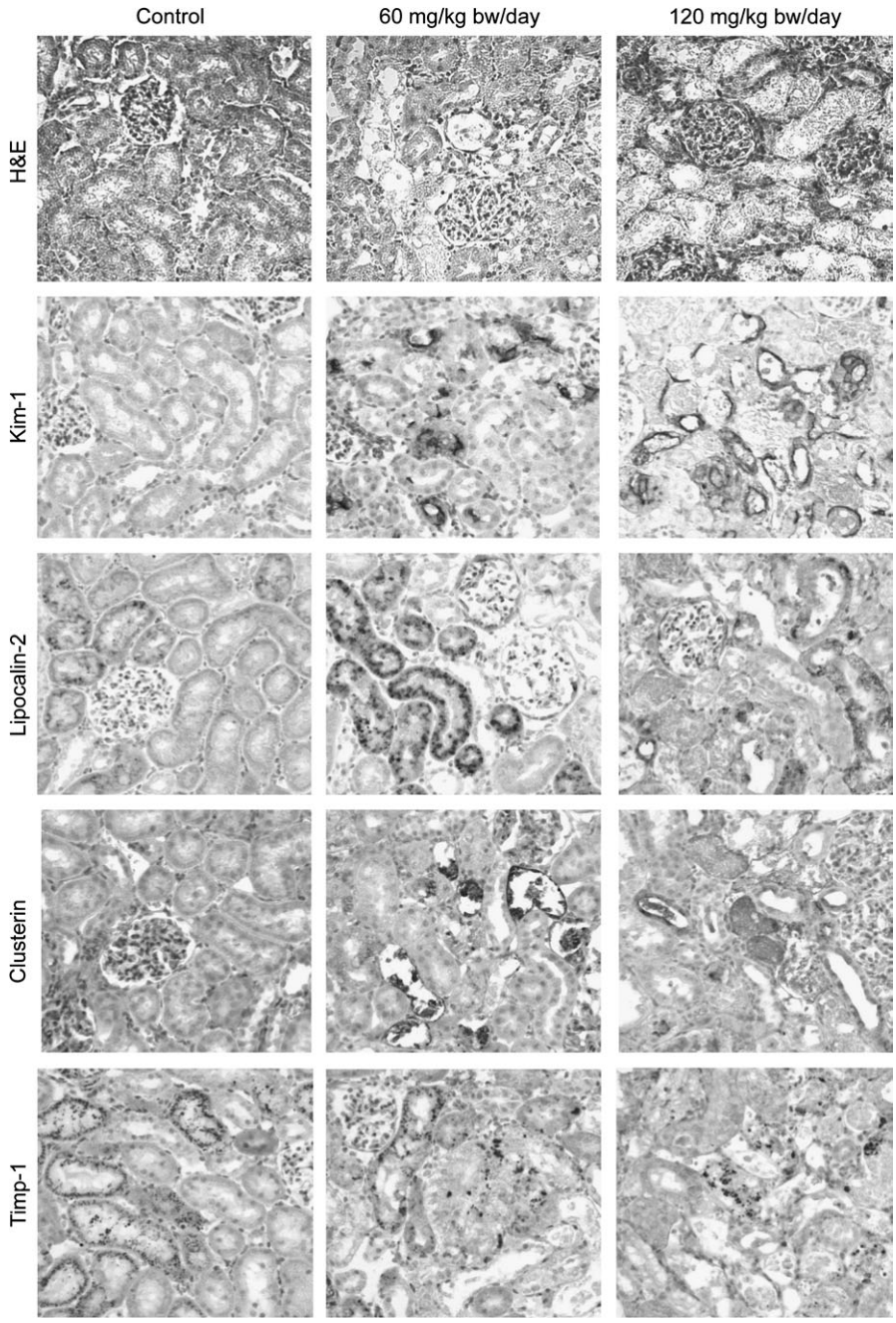

FIG. 1. Hematoxylin and eosin staining of kidney sections of Wistar rats treated with 60 and 120 mg/kg bw gentamicin for 7 days, showing marked proximal tubule cell necrosis, and immunohistochemical analysis demonstrating increased expression of Kim-1, lipocalin-2, and clusterin, but not Timp-1 within affected tubules. Kim-1 was expressed at very low levels in kidneys of untreated animals. In contrast, treatment with gentamicin resulted in a dramatic upregulation of Kim-1 in proximal tubules at the site of injury, predominantly at the apical side of flattened cells. Lipocalin-2 was evident as cytoplasmic vesicular staining within proximal tubules. Expression of lipocalin-2 in control animals was generally low but was markedly induced in response to gentamicin. Similarly, clusterin was upregulated in kidneys of gentamicin-treated rats. In line with previous reports (Hidaka *et al*., 2002; Witzgall *et al*., 1994), clusterin was predominantly detected in degenerate cells and cell debris. Timp-1 was found in intracellular vesicles of proximal tubular epithelial cells in control rat kidney. In contrast to gene expression analysis, gentamicin-mediated kidney injury did not result in increased Timp-1 immunoreactivity. Instead, an apparent loss of Timp-1–positive cells was observed.

renal tubule damage were observed as early as day 1 after treatment with 120 mg/kg bw. Marked glucosuria and proteinuria along with a decrease in osmolarity were observed in both dose groups at day 6, although statistically significant changes were generally restricted to high-dose animals (Table 1). Urinary activity of the brush boarder enzyme γ-glutamyl transferase was significantly increased in both dose groups on day 1, but not at later time points.

TABLE 2
Changes in mRNA Expression of Lipocalin-2, Clusterin, and Kim-1 in Kidneys of Rats after 7 Days of Gentamicin Treatment Using qRT-PCR

	Fold change (relative to control)		
Gene	Control	60 (mg/kg bw)	120 (mg/kg bw)
Lipocalin-2	1.0 ± 0.6	22.4 ± 12.6	99.5 ± 32.4**
Clusterin	1.0 ± 0.1	10.6 ± 7.7	22.9 ± 8.6*
Kim-1	1.0 ± 0.5	337.2 ± 94.8	1782.6 ± 570.2**
Timp-1	1.0 ± 0.2	9.2 ± 3.5**	8.9 ± 0.3**

Note. Consistent with the histopathological alterations, gentamicin treatment for 7 days resulted in a marked dose dependent increase in the expression of lipocalin-2, clusterin, timp-1, and kim-1 in kidneys. Data are presented as fold change relative to control animals. Statistical analysis was performed by ANOVA and Dunnett's *post hoc* test. Statistically significant changes compared with controls are indicated as $*p < 0.05$, $**p < 0.01$, and $***p < 0.001$.

Novel Kidney Biomarkers

Administration of 60 and 120 mg/kg bw gentamicin for 7 days resulted in increased expression of the novel kidney biomarkers Kim-1, lipocalin-2, and clusterin in the renal cortex of treated animals, as evidenced by both quantitative real-time PCR and immunohistochemistry (Table 2, Fig. 1). Timp-1 mRNA was also found to be increased, although this change was not apparent at the protein level (Table 2, Fig. 1). More importantly, however, urinary concentrations of lipocalin-2 started to increase in both dose groups as early as day 1, with statistically significant changes occurring by day 2 in both low- and high-dose animals (Fig. 2b). Analysis of urine revealed a clear time- and dose-dependent increase in urinary clusterin, which reached statistical significance by day 2 after high-dose and day 3 after low-dose treatment (Fig. 2c). Similarly, urinary Kim-1 was markedly increased in a time-and dose-dependent manner from day 1 onwards, although results were not statistically significant due to large interanimal variability (Fig. 2a). Determination of urinary Timp-1 revealed significant changes in urine obtained from rats treated with a high dose of gentamicin (120 mg/kg bw) for 3 and 6 days. ROC curves were plotted to compare the performance of novel urinary biomarkers versus traditional clinical chemistry parameters, whereby the area under the ROC curve serves as a measure for the overall ability to discriminate normal (control) versus diseased (treated) animals (Fig. 3). These analyses showed that urinary lipocalin-2 and Kim-1 appeared to be the most sensitive and specific indicators of gentamicin-induced kidney injury. In contrast, clusterin and Timp-1 were less sensitive than glucose and BUN to detect gentamicin-mediated renal toxicity. Serum creatinine and γ-glutamyl transferase were the least responsive markers of renal injury.

Metabonomics and Multivariate Data Analysis

Urine samples collected on day 1, 2, 3, and 6 after start of gentamicin treatment were subjected to ^{1}H-NMR and GC-MS analysis. Visual inspection of ^{1}H-NMR spectra and GC-MS chromatograms revealed differences in urinary composition between controls and treated animals (Fig. 4). To further investigate these differences, principal component analysis (PCA) models were constructed using ^{1}H-NMR and GC-MS data, respectively. Unsupervised multivariate data analysis of ^{1}H-NMR data showed a clear dose-dependent separation of controls and treated animals along the first principal component (PC) $t[1]$ from day 1 onwards (Fig. 5a). The shift of all high-dose and one low-dose animal on day 6 to the lower left corner of the plot along the second PC $t[2]$ shows that the biochemical composition of these urine samples differs strongly from all other samples, correlating with marked alterations in clinical chemistry parameters at this time point.

PCA of GC-MS data resulted in a model dominated by a strong outlier due to high glucose concentrations in a high-dose animal on day 6, and a cluster of control and low-dose animal moving away from the main body of samples (Fig. 5b). Analysis of the original chromatograms revealed that a large signal of the tris(trimethylsilyl) derivate of 2-oxoglutarate was responsible for the deviation of these samples in the scores plot. To obtain a homogenous data set for subsequent supervised multivariate data analysis and marker identification, these samples were excluded from the following analyses, because no analytical or biological cause could be found for this deviation. The high dose/day 6 outlier was also excluded to obtain a more homogenous data structure. The resulting PCA shown in Figure 5c demonstrates that GC-MS analysis was also able to separate treated animals from controls, although no clear time- or dose-dependent effects were evident due to a high degree of variability, presumably introduced through the sample work-up and derivatization procedure, dominating the plot.

To analyze the metabolic changes in more detail, a supervised multivariate data analysis was used. OPLS-DA models were constructed with both ^{1}H-NMR and GC-MS data, respectively (Figs. 5d and 5e). In OPLS-DA models, a classifier, in this case control, $Y = 0$, and dose, $Y = 1$ is given to each sample, and the data is modeled in such a way that the discriminating information contributing to group separation is forced onto the first PC, whereas the orthogonal information not contributing to the separation is modeled in the following components. Both ^{1}H-NMR model (Fig. 5d) and GC-MS model (Fig. 5e) show a clear separation of controls from dosed animals from day 1 onwards along the discriminating component $t[1]P$. Compared with the control groups, the dosed groups show a much larger orthogonal variance on the second orthogonal component. In particular, the high-dose animals at the late time points shift to the upper part of the plot, which is mainly driven by an increase in glucose excretion.

OPLS-DA models can aid in marker identification using the S-plot (Wiklund *et al.*, 2007). By plotting the covariance

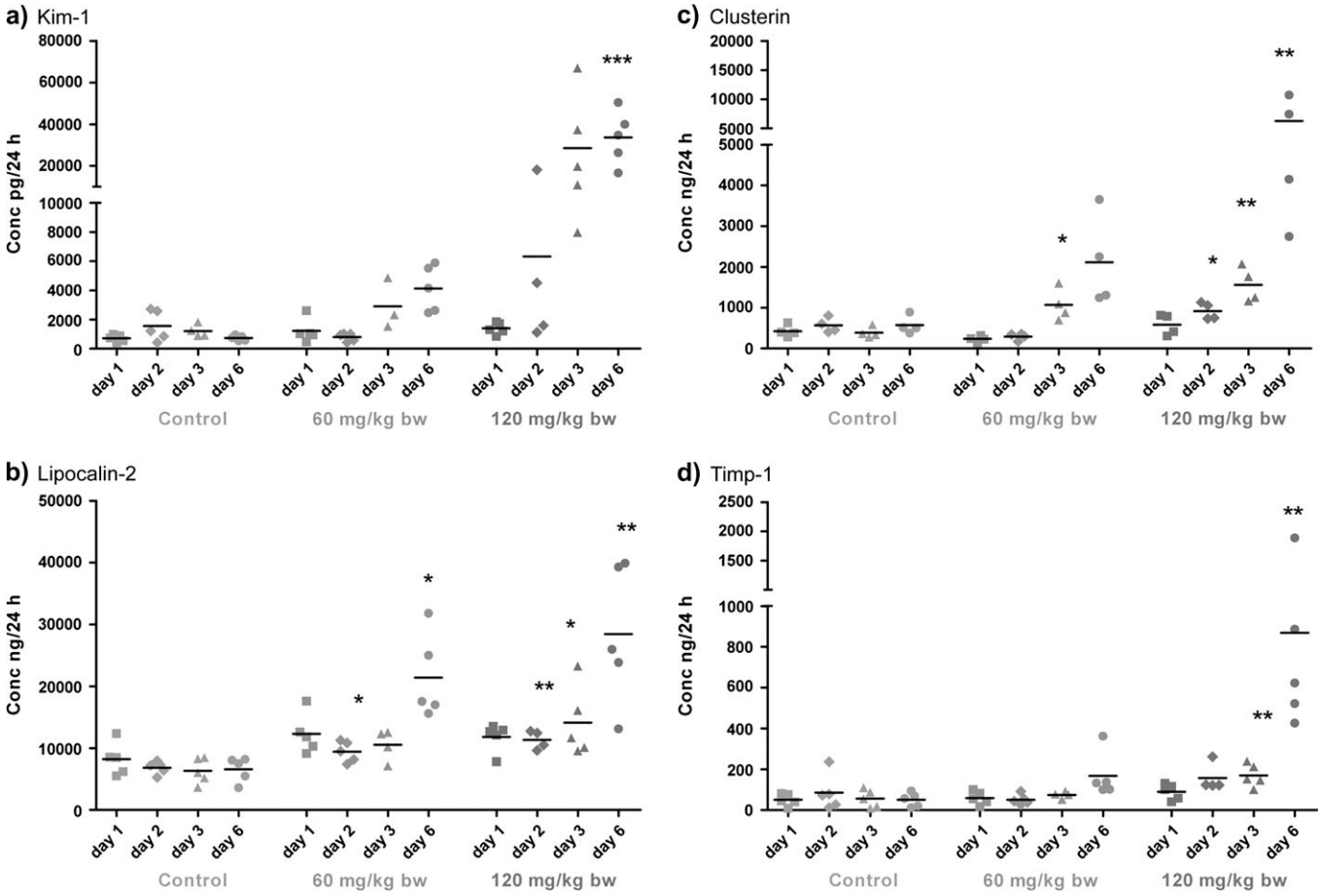

FIG. 2. Excretion of Kim 1 (a), lipocalin-2 (b), clusterin (c), and Timp-1 (d) in urine of rats treated with gentamicin (60 and 120 mg/kg bw) for 7 days. Data are presented as individual animals and mean (bar; $n = 5$). Statistical analysis was performed by ANOVA followed by Dunett′s *post hoc* test. Statistically significant changes are indicated as $*p < 0.05$, $**p < 0.01$, and $***p < 0.001$.

p against the correlation p(corr) of the variables of the discriminating component of the OPLS-DA model, an S-shaped point swarm results (data not shown). Variables which are potential markers for separating controls from dosed animals should contribute strongly to the model as described by covariance p and also correlate well with the group separation as described by p(corr). Thus, these markers are situated on the outer ends of the S-shaped curve. In our study, citrate, hippurate,

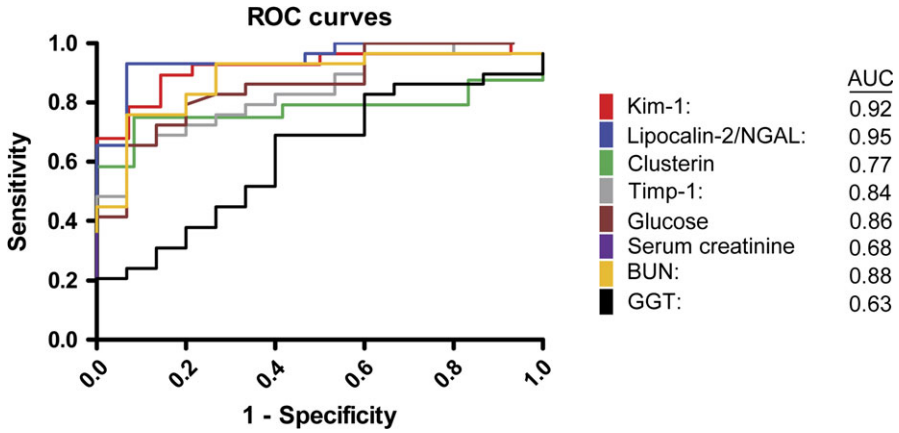

FIG. 3. ROC curves for candidate urinary biomarkers compared with traditional clinical chemistry parameters. The area under the ROC curve, which serves as measure for the overall ability of a biomarker to discriminate normal (control) versus diseased (treated) animals, is given in parenthesis.

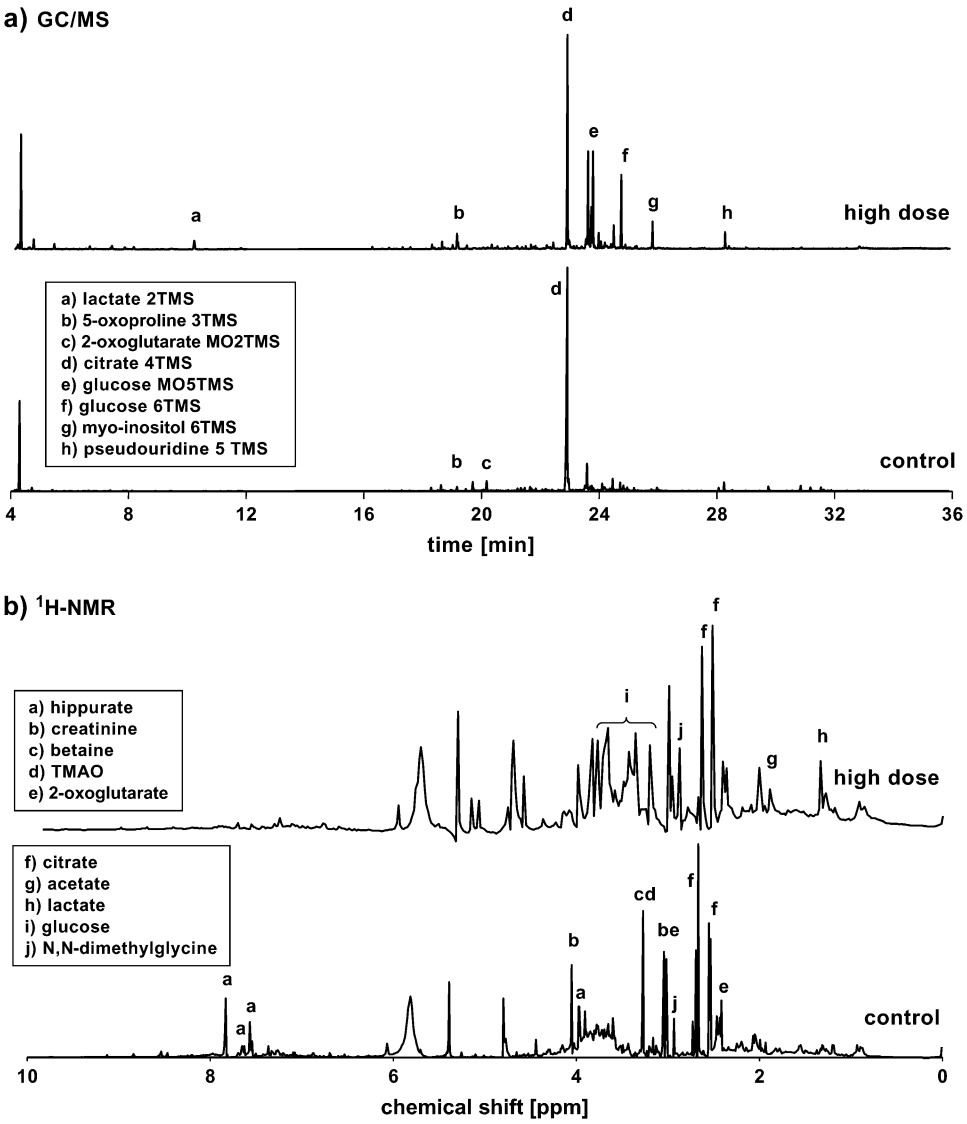

FIG. 4. Representative GC-MS chromatograms (a) and ^{1}H-NMR spectra (b) of urine obtained from control versus high-dose animals (day 6) showing metabolic changes in response to gentamicin treatment.

trigonelline, and 3-indoxylsulfate were found to be decreased in a dose-dependent manner using ^{1}H-NMR, whereas lactate, N,N-dimethylglycine and glucose increased in a dose-dependent manner (Supplementary Table 1). Several other spectral regions were also altered compared with controls, but no metabolite assignment could be made for those (Supplementary Table 1). In agreement with ^{1}H-NMR analysis, the GC-MS model showed decreased citrate and increased lactate. In addition, a decrease in 2-oxoglutarate and an increase in 5-oxoproline was observed along with alterations in aromatic gut microflora metabolites such as phenyllactate and hydroxyphenylpropionate (Table 4).

Quantitative analysis of ^{1}H-NMR spectra using the Chenomx NMR Suite database generally confirmed results obtained by multivariate data analysis (Table 3). A decrease in Krebs cycle intermediates was observed, with malonate being significantly decreased in both dose groups from day 2 onwards, whereas significant changes in citrate were only evident at individual time points in high-dose animals. A decrease in renal osmolytes, predominantly trimethylamine-N-oxide (TMAO), was also evident from day 2 onwards. Early alterations also included increased excretion of lactate and alanine, which occurred as early as day 1 in the high-dose group and on days 2 and 3 in both dose groups, and increased creatine. Hippurate, which has been associated with the gut flora, was consistently decreased in both dose-groups from day 1 onwards (Table 3).

Because alterations in gut microflora metabolites are considered to be related to the pharmacological activity of gentamicin rather than being indicative of its nephrotoxicity, further PCA and OPLS-DA models were constructed using

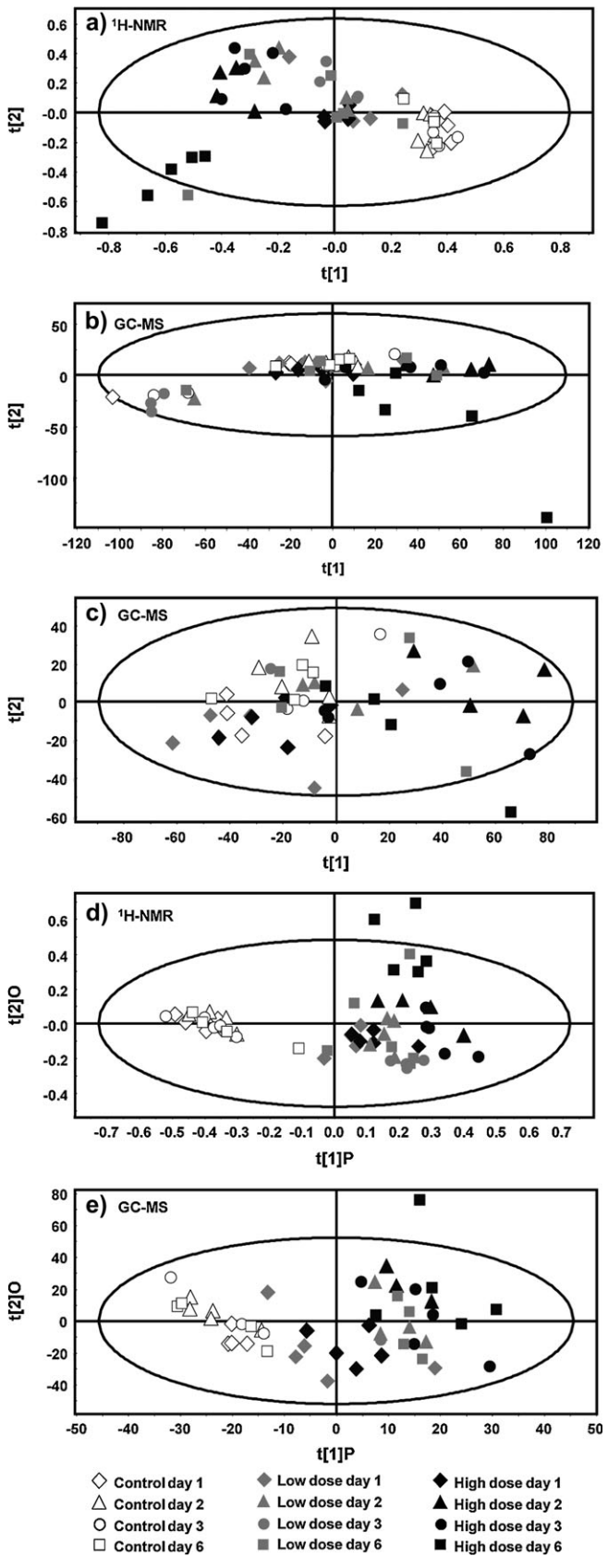

[1]H-NMR data after removal of spectral regions containing metabolites that have been linked to the gut microflora (Fig. 6). As before, a dose-dependent separation of treated from control animals was evident as early as day 1, and this separation was driven predominantly by increased glucose in response to gentamicin treatment.

DISCUSSION

The present study was designed to assess the value of a range of novel urinary biomarkers and metabonomics approaches for improved detection of kidney injury in rats using the aminoglycoside antibiotic gentamicin as a model compound.

By metabonomic analysis, a clear time- and dose-dependent separation of gentamicin-treated animals from controls was observed by PCA of [1]H-NMR data, whereas separation was less evident in the GC-MS model, in which treated animals scattered widely across the plot. Based on the [1]H-NMR OPLS-DA model, decreased citrate, hippurate, trigonelline, and 3-indoxylsulfate, and increased lactate, glucose, and N,N-dimethylglycine, were identified as major metabolic alterations responsible for the separation of control and treated animals, similar to the report by Lenz *et al.* (2005) These changes were generally confirmed by quantitative analysis, although several of these metabolites, for example, citrate, trigonelline, 3-indoxylsulfate, were found to be significantly affected only after treatment with high doses, and thus may not present sensitive indicators of gentamicin nephrotoxicity. Creatine was undetectable in urine of control animals but was excreted in urine in response to gentamicin. Although enhanced urinary creatine has previously been associated with hepatotoxicity (Connor *et al.*, 2004), it has been speculated that elevated creatine may be the result of drug induced oxidative modification of mitochondrial or cytosolic creatine kinases, enzymes susceptible to oxidative damage (Schlattner *et al.*, 2006), which is consistent with studies showing that gentamicin may induce oxidative stress and mitochondrial toxicity (Banday *et al.*, 2008; Narayana, 2008; Weinberg and Humes, 1980; Weinberg *et al.*, 1980). One of the earliest and most prominent changes induced by gentamicin treatment was the marked dose- and time-dependent decrease in hippurate. However, hippurate and several other aromatic compounds are known to present metabolites derived from the gut microflora, and its decrease after gentamicin treatment may be easily explained by the antibiotic activity of the drug. Thus, it was imperative to exclude the possibility that the PCA model was driven by the pharmacological effects of the drug, rather than by biochemical

FIG. 5. PCA score plots of [1]H-NMR (a) and GC-MS data (b), and GC-MS samples with outliers removed (c). OPLS-DA score plots of NMR (d) and GC-MS (e).

TABLE 3
Quantitative Analysis of Urinary Metabolites Detected by ^{1}H-NMR Using Chenomx NMR Suite

Dose (mg/kg bw)	Krebs cycle intermediates					Renal Osmolytes					
	Citrate	2OG	Malonate	Succinate	*cis*-Aconitate	TMAO	Betaine	Methylamine	DMG	DMA	Formate
Day 1											
0	719 ± 145	305 ± 72	22.9 ± 4.9	35.0 ± 6.2	25.9 ± 4.2	18.3 ± 5.2	18.8 ± 21.7	0.0 ± 0.0	11.8 ± 6.3	15.7 ± 1.6	12.2 ± 2.2
60	589 ± 227	280 ± 165	19.2 ± 4.1	23.3 ± 8.2	23.2 ± 6.9	13.7 ± 8.4	20.2 ± 17.9	0.6 ± 1.4	23.7 ± 9.5*	14.9 ± 6.0	9.8 ± 2.4
120	549 ± 112	296 ± 65	19.1 ± 4.6	28.5 ± 7.8	24.7 ± 4.3	16.8 ± 6.9	13.6 ± 2.9	2.9 ± 3.4	30.8 ± 3.1**	18.0 ± 2.6	9.7 ± 2.7
Day 2											
0	585 ± 104	243 ± 59	23.1 ± 5.8	49.2 ± 12.1	24.4 ± 2.2	17.1 ± 2.4	13.3 ± 13.9	3.5 ± 1.9	10.5 ± 4.9	17.2 ± 1.4	11.6 ± 2.0
60	501 ± 153	216 ± 119	11.3 ± 4.0**	27.2 ± 13.2*	18.9 ± 4.5*	5.2 ± 2.9***	11.6 ± 6.7	1.4 ± 1.4	14.6 ± 6.1	11.3 ± 4.3*	8.1 ± 2.7
120	385 ± 26*	198 ± 37	13.1 ± 3.3*	30.2 ± 10.9	18.7 ± 2.8	5.1 ± 1.9***	8.9 ± 1.5	0.7 ± 0.6*	11.7 ± 6.8	11.7 ± 2.2*	7.1 ± 2.1*
Day 3											
0	584 ± 71	245 ± 35	19.1 ± 3.9	33.1 ± 5.5	25.3 ± 3.2	19.2 ± 4.2	15.1 ± 17.4	0.8 ± 1.8	10.0 ± 6.7	16.8 ± 2.6	10.9 ± 2.2
60	560 ± 111	299 ± 59	8.0 ± 2.8***	25.8 ± 3.7	20.5 ± 2.6	5.5 ± 2.5***	19.4 ± 15.7	0.5 ± 0.6	20.0 ± 10.6	11.7 ± 2.6*	8.3 ± 1.6
120	501 ± 121	284 ± 98	10.5 ± 2.7*	23.0 ± 4.9*	15.9 ± 4.3**	2.9 ± 2.4***	9.2 ± 5.6	1.3 ± 0.8	17.1 ± 11.4	12.6 ± 2.7	6.6 ± 2.4*
Day 6											
0	650 ± 163	274 ± 56	17.9 ± 12.8	39.9 ± 6.9	31.3 ± 7.9	21.5 ± 5.9	16.8 ± 16.4	3.1 ± 2.4	9.9 ± 6.8	17.5 ± 2.6	11.9 ± 3.1
60	881 ± 164	361 ± 110	7.3 ± 13.7	36.1 ± 5.4	21.3 ± 7.5	15.4 ± 9.3	19.8 ± 18.3	0.3 ± 0.7*	18.4 ± 13.6	14.7 ± 3.9	12.0 ± 3.2
120	275 ± 186**	72 ± 51**	0.0 ± 0.0*	11.2 ± 8.3***	4.5 ± 4.8***	4.2 ± 6.1**	6.7 ± 11.9	0.2 ± 0.5*	20.3 ± 11.9	9.5 ± 4.1**	3.8 ± 2.6**

Dose (mg/kg bw)	Gut microflora metabolites											
	Hippurate	4HPA	PAG	Lactate	MNA	Acetate	Trigonelline	3IS	Alanine	Creatine	Creatinine	Glucose
Day 1												
0	142 ± 24	6.6 ± 2.9	10.6 ± 1.3	6.2 ± 1.9	2.8 ± 1.2	7.9 ± 1.1	13.6 ± 2.0	13.9 ± 3.0	3.0 ± 0.7	0.0 ± 0.0	92 ± 10	44 ± 7
60	65 ± 37**	9.6 ± 3.1	18.0 ± 6.7	7.2 ± 1.5	2.8 ± 1.1	5.5 ± 0.8*	11.7 ± 3.3	15.1 ± 3.6	3.3 ± 0.8	0.0 ± 0.0	95 ± 13	39 ± 6
120	65 ± 21**	9.3 ± 1.3	14.1 ± 7.6	18.8 ± 5.9***	2.7 ± 0.9	6.7 ± 1.8	11.9 ± 2.7	11.6 ± 7.7	7.9 ± 2.7**	0.0 ± 0.0	103 ± 10	78 ± 26
Day 2												
0	101 ± 27	10.0 ± 1.0	9.3 ± 1.9	5.5 ± 1.5	2.5 ± 1.1	13.7 ± 8.7	12.5 ± 1.8	14.6 ± 2.3	2.7 ± 0.5	0.0 ± 0.0	98 ± 14	49 ± 10
60	9 ± 3***	12.9 ± 2.9	11.3 ± 0.8	9.9 ± 1.6**	2.3 ± 0.8	6.4 ± 1.3	9.7 ± 4.8	10.2 ± 0.7	4.8 ± 1.2**	2.5 ± 2.3*	93 ± 23	49 ± 12
120	8 ± 1***	13.8 ± 1.0*	12.9 ± 2.9*	12.1 ± 1.9***	2.5 ± 1.1	6.1 ± 1.2	7.6 ± 1.8	4.3 ± 5.1***	7.2 ± 1.0***	4.9 ± 0.5***	100 ± 11	70 ± 17
Day 3												
0	105 ± 17	6.8 ± 4.5	7.9 ± 4.7	4.7 ± 0.9	2.0 ± 0.5	8.4 ± 3.6	13.3 ± 2.0	16.3 ± 2.2	2.4 ± 0.7	0.0 ± 0.0	96 ± 13	36 ± 7
60	8 ± 2***	11.2 ± 10.0	12.2 ± 3.5	9.4 ± 0.7*	2.6 ± 1.9	4.7 ± 0.9	9.9 ± 2.0	14.7 ± 2.7	3.9 ± 0.2*	0.4 ± 0.7	85 ± 11	38 ± 5
120	7 ± 2***	7.9 ± 4.5	13.6 ± 4.0	10.1 ± 3.4**	1.9 ± 0.8	5.4 ± 2.3	7.7 ± 3.1**	8.7 ± 5.5*	4.8 ± 1.2**	5.9 ± 4.7*	102 ± 25	50 ± 17
Day 6												
0	118 ± 69	10.0 ± 2.0	11.7 ± 2.2	4.9 ± 1.1	2.0 ± 0.6	11.2 ± 3.8	14.6 ± 4.0	19.3 ± 5.5	2.7 ± 0.6	0.0 ± 0.0	112 ± 20	46 ± 11
60	11 ± 4**	16.7 ± 7.5	15.0 ± 3.7	12.8 ± 2.4	2.4 ± 1.8	11.7 ± 4.0	13.1 ± 8.8	12.7 ± 9.3	4.0 ± 2.8	4.6 ± 6.3	122 ± 23	243 ± 369
120	5 ± 2**	4.7 ± 3.4	13.0 ± 4.3	21.5 ± 25.0	0.1 ± 0.2*	15.7 ± 10.2	3.1 ± 2.1*	0.3 ± 0.8***	4.1 ± 2.9	58 ± 42**	73 ± 38	382 ± 311

Note. Data are presented as mean ± SD (μmol/24 h); statistically significant changes as determined by ANOVA and Dunnett's *post hoc* test are indicated by *$p < 0.05$, **$p < 0.01$, ***$p < 0.001$. 2OG, 2-oxoglutarate; DMG, *N*,*N*-dimethylglycine; DMA, dimethylamine; 4HPA, 4-hydroxyphenylacetate; PAG, phenylacetylglycine; MNA, 1-methylnicotinamide; 3IS, 3-indoxylsulfate.

changes in response to drug toxicity. After removal of bins containing microflora associated metabolites, the resulting PCA model was still able to discriminate treated animals from controls, and was dominated by increased glucose excretion in gentamicin-treated rats. Marked glucosuria was also one of the earliest findings observed by routine clinical chemistry, and is consistent with the site-specific accumulation of aminoglycosides and subsequent damage to the S_1 and S_2 segments of the proximal tubule, which present the primary sites for glucose reabsorption.

GC-MS analysis identified alterations in several aromatic compounds such as phenyllactic acid and hydroxyphenylpropionate, which are linked to the intestinal microflora, but also an increase in urinary 5-oxoproline, an intermediate of the γ-glutamyl pathway responsible for glutathione synthesis. Increased urinary 5-oxoproline excretion has been associated with increased glutathione synthesis as a result of reactive oxygen species production (Waters *et al*., 2006), and is consistent with a range of studies pointing to a role for oxidative stress in gentamicin toxicity (Banday *et al*., 2008; Narayana, 2008). Similarly, urinary trigonelline, which was found to be decreased in response to gentamicin treatment, has been linked to glutathione depletion (Sun *et al*., 2008). The increase in lactate

TABLE 4
Metabolic Changes in Urine of Gentamicin-Treated Animals Identified by Multivariate Data Analysis of GC-MS Chromatograms

GC-MS			
Main fragments (*m/z*)	RT (s)	↑↓	Identification
117	399	↑	Lactate 2TMS
156	1123	↑	5-Oxoproline 2TMS
113, 147, 318, 347	1211	↓	2-Oxoglutarate 3TMS
193	1234	↑	Phenyllactic acid 2TMS (?)
177, 192, 205, 310	1302	↓	3-Hydroxyphenylpropionate 2TMS (?)
174	1304	↑	Putrescine 4TMS (?)
179	1326	↑	(?)
273, 347, 363, 465	1374	↓	Citrate 4TMS
192, 209	1422	↑	(?)
179	1455	↑	4-Hydroxyphenylpropionate 2TMS (?)
169, 257, 375	1785	↓	(?)
191	1892	↓	(?)

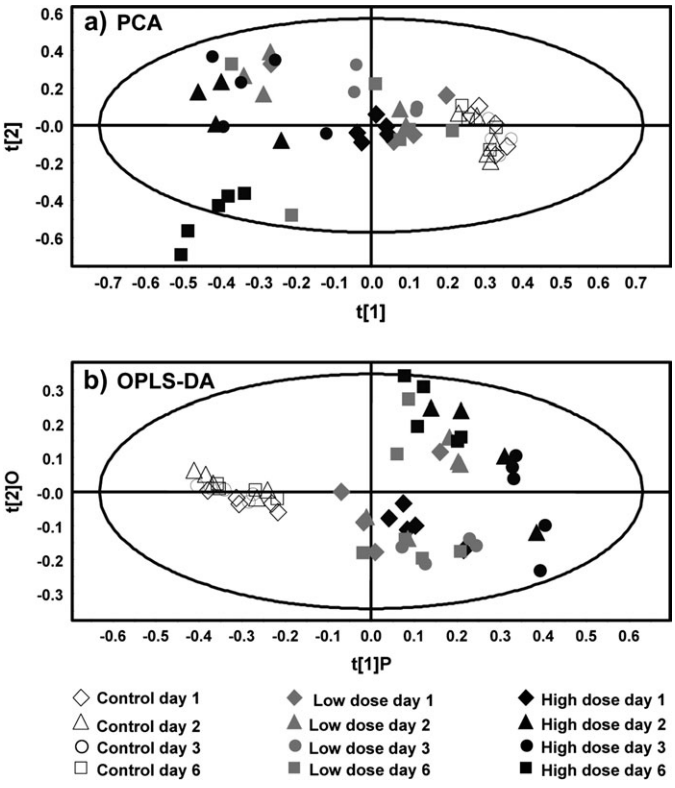

FIG. 6. PCA (a) and OPLS-DA (b) models of ^{1}H-NMR data after removal of spectral regions containing resonances associated with the gut microflora metabolites hippurate, phenylacetylglycine, and 4-hydroxyphenylacetate. S-plot analysis did not reveal additional altered bins compared with the previous models (data not shown).

excretion may be associated with impaired oxidation of pyruvate by mitochondria, consistent with the mitochondrial toxicity of gentamicin (Banday *et al*., 2008; Weinberg and Humes, 1980; Weinberg *et al*., 1980).

Although these analyses show that both NMR and GC-MS metabonomic approaches may present powerful techniques for detection of metabolic changes in response to toxicants, they also highlight the need for metabolite identification and biochemical/mechanistic interpretation to eliminate the potential of false classification based on cluster analyses, particularly when investigating pharmaceuticals which might be expected to produce some biochemical changes due to their pharmacology. At present, a major limitation of metabonomic techniques is the lack of comprehensive reference databases to aid in identification of unknown metabolites identified as being responsible for group separation within an experiment. However, even for known urinary metabolites, it needs to be recognized that the mechanistic link often remains complex and speculative, in part due to the difficulties to map the biochemical change to a specific tissue or cell type.

In contrast, protein-based urinary kidney markers were not only identified as sensitive endpoints of toxicity in this study, but their increase in urine also correlated with enhanced gene and protein expression at the site of injury. Thus, a significant advantage of a protein-based marker released into urine in response to toxic injury is that gene expression and immunolocalization can be used as valuable confirmatory tools to support urinary findings and thereby increase our confidence in the new noninvasive biomarker. Similar to our results, Kim-1 has been found to be significantly more sensitive than traditional clinical chemistry parameters in a range of models of acute and chronic kidney injury, whereby the increase in urinary Kim-1 paralleled the degree of kidney injury and Kim-1 expression in kidney (Ichimura *et al*., 2004; Prozialeck *et al*., 2007; Rached *et al*., 2008; Zhou *et al*., 2008). Important mechanistic support has come from a recent study by Ichimura *et al*. (2008) demonstrating that Kim-1 acts as a phosphatidylserine receptor which allows tubule epithelial cells to recognize and internalize apoptotic bodies and cell debris, thus preventing tubule obstruction and facilitating remodeling and regeneration of the tubule epithelium in response to injury. Because macrophages are rare within the tubule epithelium, transformation of epithelial cells into cells with phagocytic capacity through upregulation of Kim-1 appears to be an important mechanism by which dead cells are cleared from injured tubules. Collectively, these data provide substantial evidence for Kim-1 as a sensitive and specific, mechanistically anchored marker of tubule damage.

Lipocalin-2, an acute phase protein expressed by neutrophils and a variety of epithelial cells in response to inflammatory conditions and cell stress via activation of NFκB (Bu *et al*., 2006; Cowland *et al*., 2006), was also found to be significantly increased in urine of low- and high-dose animals as early as day 2, and ROC analysis suggested that lipocalin-2 outperformed even Kim-1 in the present study. Similar to Kim-1, the increase in urinary lipocalin-2 was supported by gene expression and immunohistochemistry, demonstrating upregulation in kidney

cortex of gentamicin-treated rats. These data are consistent with a range of studies which show that lipocalin-2 levels in kidney, urine or serum are altered in animal models of chemically induced tubule damage or in patients suffering from acute or chronic kidney disease (Malyszko *et al*., 2008; Mishra *et al*., 2004; Mori and Nakao, 2007; Nickolas *et al*., 2008; Wagener *et al*., 2008; Wheeler *et al*., 2008), suggesting that lipocalin-2 may serve as a sensitive marker of nephrotoxicity. However, a recent proteomics analysis of urinary markers of liver fibrosis induced by carbon tetrachloride identified lipocalin-2 as being elevated in urine of carbon tetrachloride treated animals as compared with controls (Smyth *et al*., 2008), raising concern that increased concentrations of lipocalin-2 in urine may not be as specific for kidney injury as previously thought.

Although dose- and time-dependent changes in the concentrations of urinary clusterin and Timp-1 which correlated with the progressive tubular injury in response to gentamicin treatment were evident, urinary clusterin and Timp-1 were found to be less sensitive than Kim-1 and lipocalin-2 in this study. Although urinary clusterin has been suggested to be useful to discriminate between tubular and glomerular damage (Hidaka *et al*., 2002), a recent study in patients failed to confirm these findings (Solichova *et al*., 2007). Clusterin has been implicated in a range of cellular processes, including apoptosis and growth control, cell adhesion and tissue remodeling, and has been demonstrated to be upregulated in a variety of tissues in response to cell stress (Shannan *et al*., 2006). Interestingly, urinary clusterin was also shown to be elevated in patients with bladder cancer and has been proposed as a possible laboratory marker for diagnosis of bladder cancer (Stejskal and Fiala, 2006). These data demonstrate that clusterin may be released from cell types other than kidney tubule cells and that its presence in urine may not necessarily be linked to kidney toxicity. Similar to clusterin, Timp-1 has multiple roles in cell signaling and—depending on the cellular context—may exert either anti-apoptotic or growth inhibitory activity through matrix metalloproteinase-dependent and -independent pathways (Stetler-Stevenson, 2008). Although its molecular function in kidney injury remains to be established, it is thought that Timp-1 may promote renal fibrosis through inhibition of proteolytic matrix metalloproteinases and subsequent accumulation of collagen. In addition, recent evidence suggests that Timp-1 may also contribute to kidney injury by increasing the life span of granulocytes during inflammatory conditions (Chromek *et al*., 2004).

In summary, alterations in the excretion of urinary protein biomarkers, particularly Kim-1 and lipocalin-2, were detected before marked changes in clinical chemistry parameters were evident, providing further support for the use of lipocalin-2 and Kim-1 as sensitive, mechanistically anchored biomarkers of nephrotoxicity. Although metabonomics approaches were also able to separate gentamicin-treated animals from controls and may thus be used a sensitive predictive tool, identification of discriminating metabolites and mechanistic understanding of their role in toxicity are critical.

SUPPLEMENTARY DATA

Supplementary data are available online at http://toxsci.oxfordjournals.org/.

FUNDING

Sixth Research Framework Program of the European Union (LSHB-CT-2005-518170).

ACKNOWLEDGMENTS

We are grateful to Michaela Bekteshi, Ursula Tatsch, and Elisabeth Rüb-Spiegel for excellent technical assistance. The authors would also like to thank Dr M. Grüne, Department of Organic Chemistry, University of Würzburg, for his help with recording the ^{1}H-NMR spectra.

REFERENCES

Atherton, H. J., Bailey, N. J., Zhang, W., Taylor, J., Major, H., Shockcor, J., Clarke, K., and Griffin, J. L. (2006). A combined 1H-NMR spectroscopy- and mass spectrometry-based metabolomic study of the PPAR-alpha null mutant mouse defines profound systemic changes in metabolism linked to the metabolic syndrome. *Physiol. Genomics* **27,** 178–186.

Banday, A. A., Farooq, N., Priyamvada, S., Yusufi, A. N., and Khan, F. (2008). Time dependent effects of gentamicin on the enzymes of carbohydrate metabolism, brush border membrane and oxidative stress in rat kidney tissues. *Life Sci.* **82,** 450–459.

Bennett, M., Dent, C. L., Ma, Q., Dastrala, S., Grenier, F., Workman, R., Syed, H., Ali, S., Barasch, J., and Devarajan, P. (2008). Urine NGAL predicts severity of acute kidney injury after cardiac surgery: A prospective study. *Clin. J. Am. Soc. Nephrol.* **3,** 665–673.

Bu, D. X., Hemdahl, A. L., Gabrielsen, A., Fuxe, J., Zhu, C., Eriksson, P., and Yan, Z. Q. (2006). Induction of neutrophil gelatinase-associated lipocalin in vascular injury via activation of nuclear factor-kappaB. *Am. J. Pathol.* **169,** 2245–2253.

Chromek, M., Tullus, K., Hertting, O., Jaremko, G., Khalil, A., Li, Y. H., and Brauner, A. (2003). Matrix metalloproteinase-9 and tissue inhibitor of metalloproteinases-1 in acute pyelonephritis and renal scarring. *Pediatr. Res.* **53,** 698–705.

Chromek, M., Tullus, K., Lundahl, J., and Brauner, A. (2004). Tissue inhibitor of metalloproteinase 1 activates normal human granulocytes, protects them from apoptosis, and blocks their transmigration during inflammation. *Infect. Immun.* **72,** 82–88.

Connor, S. C., Wu, W., Sweatman, B. C., Manini, J., Haselden, J. N., Crowther, D. J., and Waterfield, C. J. (2004). Effects of feeding and body weight loss on the 1H-NMR-based urine metabolic profiles of male Wistar Han rats: Implications for biomarker discovery. *Biomarkers* **9,** 156–179.

Cowland, J. B., Muta, T., and Borregaard, N. (2006). IL-1beta-specific up-regulation of neutrophil gelatinase-associated lipocalin is controlled by IkappaB-zeta. *J. Immunol.* **176,** 5559–5566.

Hidaka, S., Kranzlin, B., Gretz, N., and Witzgall, R. (2002). Urinary clusterin levels in the rat correlate with the severity of tubular damage and may help to differentiate between glomerular and tubular injuries. *Cell Tissue Res.* **310,** 289–296.

Horstrup, J. H., Gehrmann, M., Schneider, B., Ploger, A., Froese, P., Schirop, T., Kampf, D., Frei, U., Neumann, R., and Eckardt, K. U. (2002). Elevation of serum and urine levels of TIMP-1 and tenascin in patients with renal disease. *Nephrol. Dial. Transplant.* **17,** 1005–1013.

Ichimura, T., Asseldonk, E. J., Humphreys, B. D., Gunaratnam, L., Duffield, J. S., and Bonventre, J. V. (2008). Kidney injury molecule-1 is a phosphatidylserine receptor that confers a phagocytic phenotype on epithelial cells. *J. Clin. Invest.* **118,** 1657–1668.

Ichimura, T., Hung, C. C., Yang, S. A., Stevens, J. L., and Bonventre, J. V. (2004). Kidney injury molecule-1: A tissue and urinary biomarker for nephrotoxicant-induced renal injury. *Am. J. Physiol. Renal. Physiol.* **286,** F552–F563.

Ishii, A., Sakai, Y., and Nakamura, A. (2007). Molecular pathological evaluation of clusterin in a rat model of unilateral ureteral obstruction as a possible biomarker of nephrotoxicity. *Toxicol. Pathol.* **35,** 376–382.

Kharasch, E. D., Schroeder, J. L., Bammler, T., Beyer, R., and Srinouanprachanh, S. (2006). Gene expression profiling of nephrotoxicity from the sevoflurane degradation product fluoromethyl-2, 2-difluoro-1-(trifluoromethyl)vinyl ether ("compound A") in rats. *Toxicol. Sci.* **90,** 419–431.

Lenz, E. M., Bright, J., Knight, R., Westwood, F. R., Davies, D., Major, H., and Wilson, I. D. (2005). Metabonomics with 1H-NMR spectroscopy and liquid chromatography-mass spectrometry applied to the investigation of metabolic changes caused by gentamicin-induced nephrotoxicity in the rat. *Biomarkers* **10,** 173–187.

Liangos, O., Perianayagam, M. C., Vaidya, V. S., Han, W. K., Wald, R., Tighiouart, H., MacKinnon, R. W., Li, L., Balakrishnan, V. S., Pereira, B. J., *et al.* (2007). Urinary N-acetyl-beta-(D)-glucosaminidase activity and kidney injury molecule-1 level are associated with adverse outcomes in acute renal failure. *J. Am. Soc. Nephrol.* **18,** 904–912.

Lienemann, K., Plotz, T., and Pestel, S. (2008). NMR-based urine analysis in rats: Prediction of proximal tubule kidney toxicity and phospholipidosis. *J. Pharmacol. Toxicol. Methods* **58,** 41–49.

Lindon, J. C., Holmes, E., and Nicholson, J. K. (2007). Metabonomics in pharmaceutical R&D. *FEBS J.* **274,** 1140–1151.

Malyszko, J., Bachorzewska-Gajewska, H., Sitniewska, E., Malyszko, J. S., Poniatowski, B., and Dobrzycki, S. (2008). Serum neutrophil gelatinase-associated lipocalin as a marker of renal function in non-diabetic patients with stage 2-4 chronic kidney disease. *Ren. Fail.* **30,** 625–628.

Mishra, J., Ma, Q., Kelly, C., Mitsnefes, M., Mori, K., Barasch, J., and Devarajan, P. (2006). Kidney NGAL is a novel early marker of acute injury following transplantation. *Pediatr. Nephrol.* **21,** 856–863.

Mishra, J., Mori, K., Ma, Q., Kelly, C., Barasch, J., and Devarajan, P. (2004). Neutrophil gelatinase-associated lipocalin: A novel early urinary biomarker for cisplatin nephrotoxicity. *Am. J. Nephrol.* **24,** 307–315.

Mori, K., and Nakao, K. (2007). Neutrophil gelatinase-associated lipocalin as the real-time indicator of active kidney damage. *Kidney Int.* **71,** 967–970.

Narayana, K. (2008). An aminoglycoside antibiotic gentamycin induces oxidative stress, reduces antioxidant reserve and impairs spermatogenesis in rats. *J. Toxicol. Sci.* **33,** 85–96.

Nickolas, T. L., O'Rourke, M. J., Yang, J., Sise, M. E., Canetta, P. A., Barasch, N., Buchen, C., Khan, F., Mori, K., Giglio, J., *et al.* (2008). Sensitivity and specificity of a single emergency department measurement of urinary neutrophil gelatinase-associated lipocalin for diagnosing acute kidney injury. *Ann. Intern. Med.* **148,** 810–819.

Odunsi, K., Wollman, R. M., Ambrosone, C. B., Hutson, A., McCann, S. E., Tammela, J., Geisler, J. P., Miller, G., Sellers, T., Cliby, W., *et al.* (2005). Detection of epithelial ovarian cancer using 1H-NMR-based metabonomics. *Int. J. Cancer* **113,** 782–788.

Prozialeck, W. C., Vaidya, V. S., Liu, J., Waalkes, M. P., Edwards, J. R., Lamar, P. C., Bernard, A. M., Dumont, X., and Bonventre, J. V. (2007). Kidney injury molecule-1 is an early biomarker of cadmium nephrotoxicity. *Kidney Int.* **72,** 985–993.

Rached, E., Hoffmann, D., Blumbach, K., Weber, K., Dekant, W., and Mally, A. (2008). Evaluation of putative biomarkers of nephrotoxicity after exposure to ochratoxin a in vivo and in vitro. *Toxicol. Sci.* **103,** 371–381.

Sangster, T., Major, H., Plumb, R., Wilson, A. J., and Wilson, I. D. (2006). A pragmatic and readily implemented quality control strategy for HPLC-MS and GC-MS-based metabonomic analysis. *Analyst* **131,** 1075–1078.

Schlattner, U., Tokarska-Schlattner, M., and Wallimann, T. (2006). Mitochondrial creatine kinase in human health and disease. *Biochim. Biophys. Acta* **1762,** 164–180.

Shannan, B., Seifert, M., Leskov, K., Willis, J., Boothman, D., Tilgen, W., and Reichrath, J. (2006). Challenge and promise: Roles for clusterin in pathogenesis, progression and therapy of cancer. *Cell Death Differ.* **13,** 12–19.

Smyth, R., Lane, C. S., Ashiq, R., Turton, J. A., Clarke, C. J., Dare, T. O., York, M. J., Griffiths, W., and Munday, M. R. (2008). Proteomic investigation of urinary markers of carbon-tetrachloride-induced hepatic fibrosis in the Hanover Wistar rat. *Cell Biol. Toxicol.* [Epub ahead of print], DOI:10.1007/s10565-008-9104-8.

Solichova, P., Karpisek, M., Ochmanova, R., Hanulova, Z., Humenanska, V., Stejskal, D., and Bartek, J. (2007). Urinary clusterin concentrations–a possible marker of nephropathy? Pilot study. *Biomed. Pap. Med. Fac. Univ. Palacky Olomouc Czech. Repub.* **151,** 233–236.

Stejskal, D., and Fiala, R. R. (2006). Evaluation of serum and urine clusterin as a potential tumor marker for urinary bladder cancer. *Neoplasma* **53,** 343–346.

Stetler-Stevenson, W. G. (2008). Tissue inhibitors of metalloproteinases in cell signaling: Metalloproteinase-independent biological activities. *Sci. Signal.* **1,** re6.

Sun, J., Schnackenberg, L. K., Holland, R. D., Schmitt, T. C., Cantor, G. H., Dragan, Y. P., and Beger, R. D. (2008). Metabonomics evaluation of urine from rats given acute and chronic doses of acetaminophen using NMR and UPLC/MS. *J. Chromatogr. B Anal. Technol. Biomed. Life Sci.* **871,** 328–340.

Vaidya, V. S., Bobadilla, N. A., and Bonventre, J. V. (2005). A microfluidics based assay to measure kidney injury molecule-1 (Kim-1) in the urine as a biomarker for early diagnosis of acute kidney injury. *J. Am. Soc. Nephrol.* **16,** 192.

Vaidya, V. S., Waikar, S. S., Ferguson, M. A., Collings, F. B., Sunderland, K., Gioules, C., Bradwin, G., Matsouaka, R., Betensky, R. A., Curhan, G. C., *et al.* (2008). Urinary biomarkers for sensitive and specific detection of acute kidney injury in humans. *Clin. Transl. Sci.* **1,** 200–208.

van Timmeren, M. M., Vaidya, V. S., van Ree, R. M., Oterdoom, L. H., de Vries, A. P., Gans, R. O., van Goor, H., Stegeman, C. A., Bonventre, J. V., and Bakker, S. J. (2007). High urinary excretion of kidney injury molecule-1 is an independent predictor of graft loss in renal transplant recipients. *Transplantation* **84,** 1625–1630.

Wagener, G., Gubitosa, G., Wang, S., Borregaard, N., Kim, M., and Lee, H. T. (2008). Urinary neutrophil gelatinase-associated lipocalin and acute kidney injury after cardiac surgery. *Am. J. Kidney Dis.* **52,** 425–433.

Want, E. J., O'Maille, G., Smith, C. A., Brandon, T. R., Uritboonthai, W., Qin, C., Trauger, S. A., and Siuzdak, G. (2006). Solvent-dependent metabolite distribution, clustering, and protein extraction for serum profiling with mass spectrometry. *Anal. Chem.* **78,** 743–752.

Wasilewska, A. M., and Zoch-Zwierz, W. M. (2008). Urinary levels of matrix metalloproteinases and their tissue inhibitors in nephrotic children. *Pediatr. Nephrol.* **23,** 1795–1802.

Waters, N. J., Waterfield, C. J., Farrant, R. D., Holmes, E., and Nicholson, J. K. (2006). Integrated metabonomic analysis of bromobenzene-induced hepatotoxicity: Novel induction of 5-oxoprolinosis. *J. Proteome Res.* **5,** 1448–1459.

Wei, L., Liao, P., Wu, H., Li, X., Pei, F., Li, W., and Wu, Y. (2008). Toxicological effects of cinnabar in rats by NMR-based metabolic profiling of urine and serum. *Toxicol. Appl. Pharmacol.* **227,** 417–429.

Weinberg, J. M., Harding, P. G., and Humes, H. D. (1980). Mechanisms of gentamicin-induced dysfunction of renal cortical mitochondria. II. Effects on

mitochondrial monovalent cation transport. *Arch. Biochem. Biophys.* **205,** 232–239.

Weinberg, J. M., and Humes, H. D. (1980). Mechanisms of gentamicin-induced dysfunction of renal cortical mitochondria. I. Effects on mitochondrial respiration. *Arch. Biochem. Biophys.* **205,** 222–231.

Wheeler, D. S., Devarajan, P., Ma, Q., Harmon, K., Monaco, M., Cvijanovich, N., and Wong, H. R. (2008). Serum neutrophil gelatinase-associated lipocalin (NGAL) as a marker of acute kidney injury in critically ill children with septic shock. *Crit. Care Med.* **36,** 1297–1303.

Wiklund, S., Johansson, E., Sjostrom, L., Mellerowicz, E. J., Edlund, U., Shockcor, J. P., Gottfries, J., Moritz, T., and Trygg, J. (2007). Visualization of GC/TOF-MS-based metabolomics data for identification of biochemically interesting compounds using OPLS class models. *Anal. Chem.* **80,** 116–123.

Williams, R., Lenz, E. M., Wilson, A. J., Granger, J., Wilson, I. D., Major, H., Stumpf, C., and Plumb, R. (2006). A multi-analytical platform approach to the metabonomic analysis of plasma from normal and Zucker (fa/fa) obese rats. *Mol. Biosyst.* **2,** 174–183.

Witzgall, R., Brown, D., Schwarz, C., and Bonventre, J. V. (1994). Localization of proliferating cell nuclear antigen, vimentin, c-Fos, and clusterin in the postischemic kidney. Evidence for a heterogenous genetic response among nephron segments, and a large pool of mitotically active and dedifferentiated cells. *J. Clin. Invest.* **93,** 2175–2188.

Yang, A., Trajkovic, D., Illanes, O., and Ramiro-Ibanez, F. (2007). Clinicopathological and tissue indicators of para-aminophenol nephrotoxicity in Sprague-Dawley rats. *Toxicol. Pathol.* **35,** 521–532.

Zhou, Y., Vaidya, V. S., Brown, R. P., Zhang, J., Rosenzweig, B. A., Thompson, K. L., Miller, T. J., Bonventre, J. V., and Goering, P. L. (2008). Comparison of kidney injury molecule-1 and other nephrotoxicity biomarkers in urine and kidney following acute exposure to gentamicin, mercury, and chromium. *Toxicol. Sci.* **101,** 159–170.